BL-3A, BL-4C, BL-8B/ 2019G557

Short correlation of Eu valence order in layered compound $Eu_3Bi_2S_4F_4$

Kazuaki IWASA[1,*], Hironori NAKAO[2], Hajime SAGAYAMA[2],
Ryuji HIGASHINAKA[3], Ryotaro SAKATANI[3], Tatsuma D. MATSUDA[3], and Yuji AOKI[3]
[1] Research and Education Center for Atomic Sciences, Ibaraki University, Tokai, Naka, Ibaraki 319-1106, Japan.
[2] Institute of Materials Structure Science, High Energy Accelerator Research Organization, Tsukuba, Ibaraki 305-0801, Japan
[3] Department of Physics, Tokyo Metropolitan University, Tokyo 192-0397, Japan

X-ray measurements were performed to investigate the crystal structure of $Eu_3Bi_2S_4F_4$, which is reported to be a superconductor in the antiferromagnetic ordered phase. The X-ray diffraction profile revealed a short correlation length of the crystal lattice along the tetragonal *c* axis, which is a signature of the stacking fault of the BiS_2 and Eu_3Bi_4 layers. The short-length correlation is expected to comprise the Eu-ion valence order because the resonant peak was observed at the Eu L_3 absorption edge on the diffuse scattering.

1 Introduction

The BiS_2-based superconductors are an attractive material series, which are characterized by the layered structure and the systematic variation with the rare-earth elements [1]. The rare-earth elements form the layer with oxygen or fluorine, and this layer become carrier doner to the conductive the BiS_2 layers.

$Eu_3Bi_2S_4F_4$ was discovered to be a superconductor below T_C = 1.5 K that appears simultaneously with an antiferromagnetic ordering at 2.3 K [2]. Figure 1 shows the crystal structure of $Eu_3Bi_2S_4F_4$, which was drawn using the VESTA software [3]. The lattice constants of $Eu_3Bi_2S_4F_4$, which crystalizes in a tetragonal structure with the space group of *I*4/*mmm* (No. 139), at room temperature are a = 4.0748(11) Å, c = 32.340(9) [4]. Eu and F atoms form layered structure, which sandwich layers comprising Bi and S, as described above.

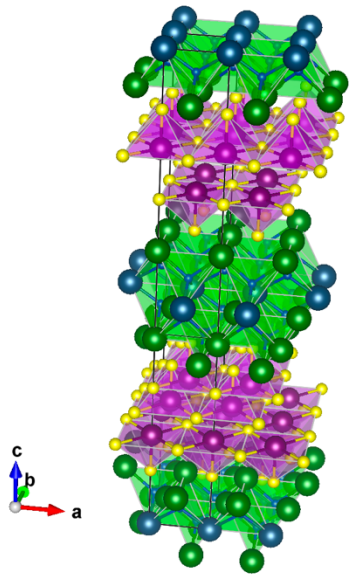

Fig. 1: Crystal structure of $Eu_3Bi_2S_4F_4$. Green, blue purple, and yellow circles are Eu, F, Bi, and S atoms, respectively. The figure is drawn using the VESTA software [3].

The electrical resistivity of $Eu_3Bi_2S_4F_4$ exhibits an anomalous temperature dependence. The paper on 2014 reported less temperature dependence of the resistivity above T_C [2]. In contrast, the paper on 2023 reported a drastic increase of resistivity by a factor of approximately 10^3 on decreasing temperature from 300 K to T_C [5]. The huge low-temperature resistivity is suppressed by applying pressures. Moreover, the recent data shows the enhancement by a factor of approximately 10^7 [6]. These two conflicted resistivity behaviors, reported in the individual papers, give a motivation to understand the carrier state in view of crystallography.

2 Experiment

Synchrotron X-ray diffraction measurements of a single-crystalline sample of $Eu_3Bi_2S_4F_4$ were performed using the four-circle diffractometer installed at BL-3A, 4C, and 8B of the Photon Factory (PF) in KEK. In the measurements at BL-3A, magnetic field effects were examined, using a superconducting magnet cryostat. The experiment at BL-4C was performed using a helium-closed refrigerator. X-ray absorption spectra (XAS) was also measured at BL-4C. We also performed X-ray diffraction experiment at the oscillating photograph diffractometer at BL-8B equipped with a helium-closed refrigerator in the Photon Factory in KEK.

3 Results and Discussion

The X-ray absorption spectrum (XAS) was measured using a silicon drift detector at BL-4C. Figure 2 shows the XAS near the L3 absorption edge of $Eu_3Bi_2S_4F_4$ at 4 and 280 K, corresponding to the fluorescence of $L\alpha$ radiation. temperatures. The peaks at 6.973 and 6.981 keV are attributed to the X-ray emissions of Eu ions. Previous study on the XAS also revealed the similar two-peak spectrum [7]. Further, the similar two components were also identified for the Eu-ion charge ordering behavior of Eu_3S_4 [8] and Eu_3As_4 [9]. These features are explained by a mixed valence state of Eu^{2+} and Eu^{3+}. The green and blue

solid lines in Fig. 2 are calculated XAS spectra for Eu^{2+} and Eu^{3+}, respectively, which are assumed to be summation of a Lorentzian peak and an arctangent component. The XAS data was analyzed by a least-squares fitting procedure based on combination of calculated spectra for Eu^{2+} and Eu^{3+}. The solid lines on the measured data are the fitted results, which reproduce the data well.

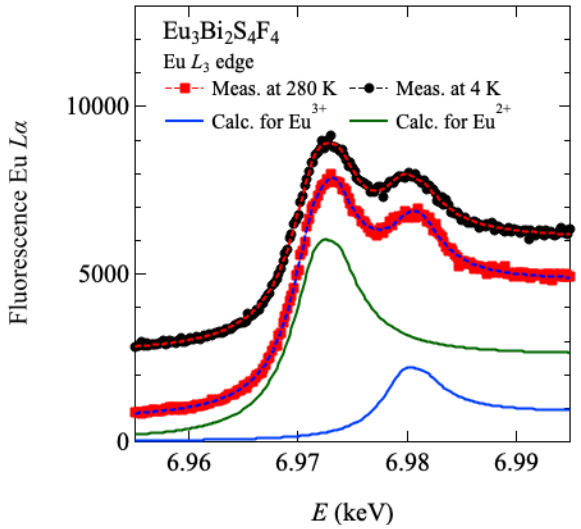

Fig. 2: XAS spectra corresponding to $L\alpha$ fluorescence intensity near the Eu L_3 edge absorption in $Eu_3Bi_2S_4F_4$.

Figure 3 shows the peak position of two components (red squares and black circles) and a intensity ratio between the Eu^{2+} and Eu^{3+} components (blue triangles). These data do not show clear temperature dependences within the experimental errors. The ratio in present study is approximately 3.2, which indicates the average valence of Eu is $(3.2 \times 2 + 1.0 \times 3)/(3.2 + 1.0) \simeq 2.2$, which is consistent with the previous study [7].

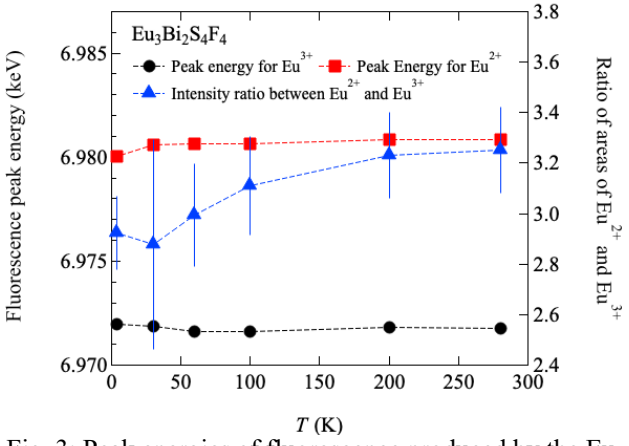

Fig. 3: Peak energies of fluorescence produced by the Eu L_3 edge absorption.

We performed X-ray diffraction measurements to reveal structural features of $Eu_3Bi_2S_4F_4$, using the BL-8B and BL-4C instruments. Figure 4 shows an oscillation photograph for the single crystalline sample at room temperature, obtained using BL-8B. The strong peaks were observed, as indicated by the Miller indices for the crystal structure of $Eu_3Bi_2S_4F_4$, as shown in Fig. 1. These fundamental peaks are slightly broader along the Debye–Scherrer ring direction (nearly vertical direction in Fig. 4). In addition, diffuse intensities are detected, as indicated by green circles, which are just at the middle points between the fundamental reflections. The diffuse scattering is characterized by the propagation vector $\boldsymbol{q}$ = (1/2, 1/2, 0). The peak distribution along the [0 0 1] axis (horizontal direction in Fig. 4) is broader, while the width along the [1 1 0] axis is narrower. Such anistropic diffuse scattering indicates that the short correlation length along the [0 0 1] axis, and the doubling of the structural unit along the [1 1 0] axis is rather in long range.

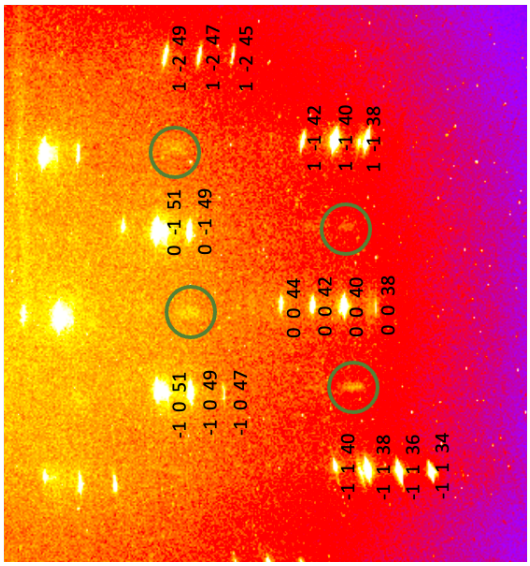

Fig. 4: An oscillation photograph of $Eu_3Bi_2S_4F_4$, measured at BL-8B.

Figure 5 shows the diffraction patterns along the [1, 1, L] axis (black circles) and the [0, 0, L] axis (red squares), measured at the four-circle diffractometer at BL-4C of PF. The strong fundamental peaks are located at $\boldsymbol{Q}$ = (1, 1, L) and (0, 0, L) with L = even for the tetragonal structure with the space group of $I4/mmm$ (No. 139). The intensity of the fundamental peak at $\boldsymbol{Q}$ = (0, 0, 10) was approximately 1.257×10^7 in unit of Fig. 5, which are not shown because of the strong intensity was not measured using the same diffractometer condition (the attenuators). The same order of magnitude of diffraction intensities were observed at $\boldsymbol{Q}$ = (1, 1, L) and (0, 0, L) with L = even. Additionally, we detected sharp peaks at $\boldsymbol{Q}$ = (0, 0, 4.8), (0, 0, 7.2), (0, 0, 9.6), (0, 0, 14.2), and (0, 0, 16.8), which are not consistent with the Bragg peaks expected for $Eu_3Bi_2S_4F_4$. These additional reflections are explained by the reciprocal lattice points (0, 0, L) with L = integers between 2 and 7 of $EuBiS_2F$, as indicated by the green lines. The lattice constants of $EuBiS_2F$ at 13 K, which crystalizes in a tetragonal structure with the space group of $P4/nmm$ (No. 129), are a = 4.0408(1) Å and c = 13.4767(3) Å [10]. This result indicates that the sample contains an impurity phase

of $EuBiS_2F$. The intensity at $\boldsymbol{Q}$ = (0, 0, 9.6), corresponding to the diffraction for $\boldsymbol{Q}$ = (0, 0, 4) of $EuBiS_2F$, is 8.038 × 10^5 counts, which is approximately 6.4% of the intensity at $\boldsymbol{Q}$ = (0, 0, 10) of $Eu_3Bi_2S_4F_4$. Therefore, the volume ratio of $EuBiS_2F$ to $Eu_3Bi_2S_4F_4$ is in order of 10^{-2}.

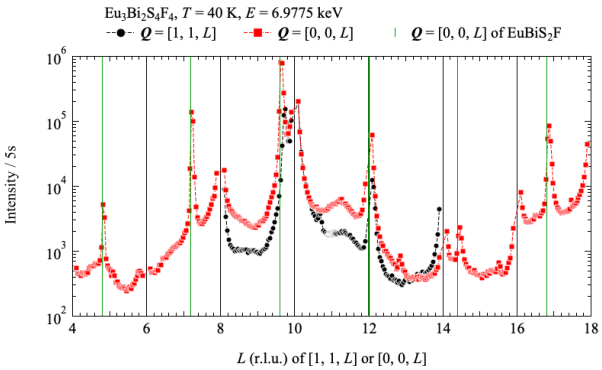

Fig. 5: Diffraction patterns along the [1, 1, L] axis (black circles) and the [0, 0, L] axis (red squares). The abscissa is in unit of the reciprocal lattice of $Eu_3Bi_2S_4F_4$. The green lines indicate the reciprocal lattice points (0, 0, L) with L = integers of $EuBiS_2F$.

Additionally, diffuse scattering intensity is superimposed to the sharp Bragg peaks in both scans along the [1, 1, L] axis (black circles) and the [0, 0, L] axis (red squares). This fact indicates that the crystal structure of the present sample is characterized not only by the mixing of $Eu_3Bi_2S_4F_4$ and $EuBiS_2F$, but also by a short correlation length along the crystallographic c axis, which corresponds to stacking fault of atomic layers. The crystal structures of $Eu_3Bi_2S_4F_4$ and $EuBiS_2F$ resemble each other because, simply saying, both compounds comprise the BiS_2 and Eu_3F_4 layers. The stacking sequence of these two layers are slightly different from each other, resulting in the inequivalent unit-cell c axis. Moreover, the stacking sequence patterns of the BiS_2 and Eu_3F_4 layers are not discrete and various stacking patterns may be allowed in the present single crystalline sample.

To deduce the short correlation length more in detail, we performed resonant X-ray scattering measurements at $\boldsymbol{Q}$ = (0.5, 0.5, L) because this Q region corresponds to the diffuse scattering positions observed in the oscillation photograph shown in Fig. 1. Figure 6 shows the scans along the [0.5, 0.5, L] axis measured at 3 K (black circles) and 280 K (red squares). Filled marks are data measured at E = 6.9775 keV just on the Eu L_3 edge energy, and open marks are data measured at E = 6.9000 keV. Despite that the scan region in the reciprocal space is the Brillouin zone boundary of $Eu_3Bi_2S_4F_4$, a clear L dependence in the broad scattering intensity is seen. Therefore, as observed in the scans along the [1, 1, L] and [0, 0, L] axes, the data evidence the short correlation stacking along the c axis. The similar patterns at 3 and 280 K reveal that the structural short correlation is robust against temperatures. Furthermore, the broad peak feature is apparently enhanced in the measurement at the Eu L_3 edge energy at E = 6.9775 keV, compared to the data taken at E = 6.9000 keV.

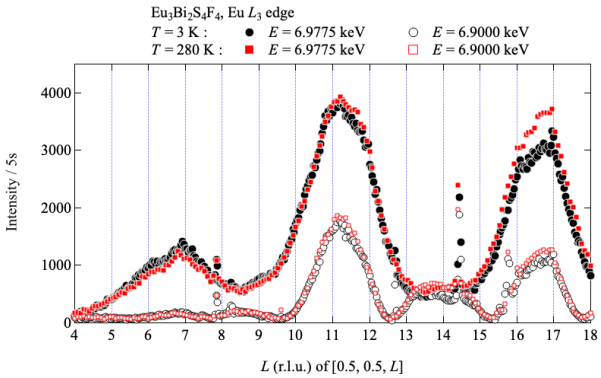

Fig. 6: Diffraction patterns along the [0.5, 0.5, L] axis measured at 3 K (black circles) and 280 K (red squares). Filled marks are measured at E = 6.9775 keV (the Eu L_3 edge energy), and open marks are measured at E = 6.9000 keV.

Figure 7 shows incident X-ray energy dependence of the diffuse scattering intensity at $\boldsymbol{Q}$ = (0.5, 0.5, 11), where the maximum intensity appears along the [0.5, 0.5, L] axis, as shown in Fig. 5. It is notable that a clear resonant peak appears at E = 6.977 keV, which is just between the XAS peaks for Eu^{2+} and Eu^{3+}, as shown Fig. 2. The similar feature of the resonant spectrum was reported for the Yb L_3-edge reflection in the charge ordered phase of Yb_4As_3 [7], where the Yb sites split to Yb^{2+} and Yb^{3+} ions. Therefore, the present resonant spectra for $Eu_3Bi_2S_4F_4$ indicates that Eu^{2+} and Eu^{3+} exhibit a charge ordered structure with short correlation length.

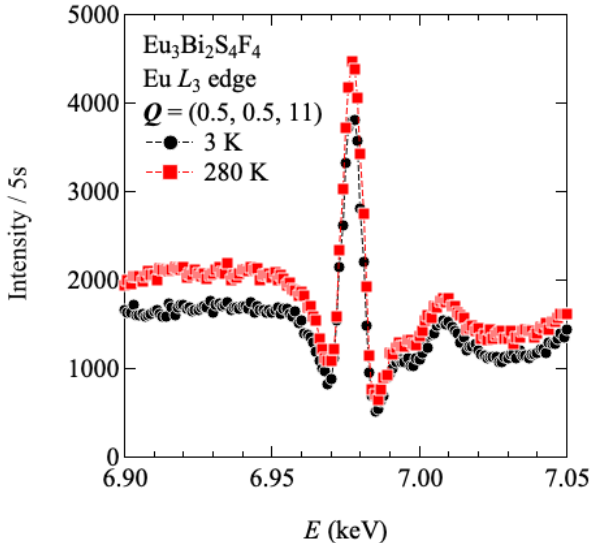

Fig. 7: Incident energy dependence of diffraction intensity at the fixed scattering vector $\boldsymbol{Q}$ = (0.5, 0.5, 11) of $Eu_3Bi_2S_4F_4$ at 3 K (black circles) and 280 K (red squares).

We measured magnetic field dependence of the resonant spectrum, using the cryomagnet at BL-3A. Under the magnetic fields to 2.25 T applied along the crystallographic [1, –1, 0] axis, no significant dependence on magnetic fields was observed at 1.7 K. This fact indicates that the correlation between the Eu^{2+} and Eu^{3+}

ions is robust against magnetic fields, despite the Eu^{2+} ions possess magnetic degrees of freedom associated with the J = 7/2 total angular momentum state and the nonmagnetic Eu^{3+} ions.

4 Summary

The structural short correlation accompanied by the correlation of Eu^{2+} and Eu^{3+} ions are indicated from the present synchrotron X-ray scattering experiments. This charge ordering behavior, independent of temperature and magnetic field, indicates that conductive carriers, supposed to be provided from the Eu_3F_4 layers to the BiS_2 layers, are localized owing to the imperfect crystal structure. This scenario seems to be consistent with the semiconductive behavior in electrical resistivity of the same sample batch used in the present diffraction study [6]. The variation of magnitude of electrical resistivities, reported independently by several research groups, is caused by the sample dependence on crystal lattice property, which is characterized by the stacking sequence of the BiS_2 and Eu_3F_4 layers and correlation lengths. At present, we have not yet solved detailed structure of the short-correlation charge ordered state of the Eu ions. The structure may relate with the mixed crystal of $Eu_3Bi_2S_4F_4$ and $EuBiS_2F$ because the stacking fault of atomic layers are expected from the similarity of crystal structures of both compounds.

Acknowledgement

The present study was performed under the allocated proposal for the photon Factory (2019G557).

References

[1] S. Demura, Nov. Supercond. Mater. **2**, 1 (2016).
[2] Hui-Fei Zhai et al., J. Am. Chem. Soc. **136**, 15386 (2014).
[3] K. Momma and F. Izumi, J. Appl. Crystallogr. **41**, 653 (2008).
[4] R. Higashinaka et al., Physica B **536** (2018) 824.
[5] K. Ishigaki et al., JPS Conf. Proc. **38**, 011101 (2023).
[6] R. Higashinaka et al., Phys. Rev. B **108**, L081122 (2023).
[7] E. Paris et al., Phys. Rev. B **95**, 035152 (2017).
[8] H. Ohara et al., Physica B **350**, 353 (2004).
[9] H. Nakao et al., J. Phys. Chem. Solids **68**, 2064 (2007).
[10] Hui-Fei Zhai et al., Phys. Rev. B **90**, 064518 (2014).

* kazuaki.iwasa.ifrc@vc.ibaraki.ac.jp